

# Cooling Effects on a Model Rennet Casein Gel System: Part I. Rheological Characterization

Qixin Zhong,<sup>†,‡</sup> Christopher R. Daubert,<sup>\*,†</sup> and Orlin D. Velev<sup>‡</sup>

Department of Food Science, North Carolina State University,  
Raleigh, North Carolina 27695, and Department of Chemical Engineering,  
North Carolina State University, North Carolina 27695

Received November 14, 2003. In Final Form: June 10, 2004

The gelation of a model rennet casein system was studied during cooling at different rates. During cooling, casein network structure development was proposed to evolve over a few steps at different length scales: molecules, particles, flocs, or network. Rennet casein flocs are fractal in nature, and fractal dimension and floc size are two variables affecting the rheology and microstructure of a rennet casein gel. Casein structure formation during cooling from 80 to 5 °C at four different rates (0.5, 0.1, 0.05, and 0.025 °C/min) was monitored by dynamic rheological tests, and a stronger gel developed at a slower cooling rate. During different cooling schedules, similar fractal dimensions were observed due to a lack of difference in the colloidal interactions. Differences among rheological data were possibly caused by variability in floc size, as observed in the second part of this paper. A larger number of smaller-sized flocs enabled gelation at a higher temperature and created a stronger network at a slower cooling rate. Controlling cooling schemes thus provides an approach for manipulating casein gelation and the microstructure for a system of fixed chemical compositions.

## Introduction

Casein forms a continuous network in a large variety of dairy products. In bovine milk, casein consists of ~80% proteins and has four generic variances:  $\alpha$ ,  $\beta$ ,  $\kappa$ , and  $\gamma$ .<sup>1,2</sup> Caseins in milk do not exist as single macromolecules but aggregate into micelles. Thousands of casein molecules exist inside the micelle even though the manner by which these molecules are arranged into structures is still debated.<sup>3–5</sup> Casein molecules in the micelle are calcium sensitive, and the structure of casein micelles is sustained by the calcium phosphate complexes linking these proteins, possibly in addition to hydrophobic interactions.<sup>1</sup>

Processed cheese is an important dairy product. Production of processed cheese involves mixing natural cheeses with emulsifying salts at an elevated temperature with agitation, followed by cooling.<sup>6</sup> The added emulsifying salts, for example, disodium phosphate and monosodium phosphate, sequester calcium inside the casein micelles, disintegrating casein micelles into smaller units and thereby increasing protein solubility.<sup>7–9</sup> Caseins exist as a mixture of individual molecules and form a continuous network upon cooling at the last stage of processed cheese

manufacturing. However, there is a lack of information on the network formation process from this casein mixture.

Protein and fat are two major components of processed cheese. Fat crystallization, protein–protein interactions, and protein–fat interactions are important factors contributing to structure formation upon cooling.<sup>6</sup> A faster cooling rate generates smaller fat crystals<sup>10</sup> and a higher solid fat content,<sup>11</sup> potentially generating a firmer cheese.<sup>12</sup> Nevertheless, a slower cooling rate has been observed to generate a firmer cheese.<sup>7</sup> Therefore, studies on protein–protein interactions during cooling may help interpret the mechanisms by which cooling affects processed cheese functionality.

The objective of this work was to study casein gelation as well as cooling rate effects. To fulfill this objective, a model system was formulated to have a composition similar to a processed cheese analogue.<sup>9,13,14</sup> Casein powder produced from renneting, with a similar casein composition to that of natural cheeses, was used as the protein source, and monosodium and disodium phosphates were used as the emulsifying salts. Experiments with the model rennet casein system cooled at different rates were performed. Fractal theory was used to describe protein structure formation, and fractal dimension and floc size were treated as two variables potentially affecting the rheology and microstructure of a rennet casein gel. The scaling theory developed by Shih et al.<sup>15</sup> was adopted to determine the fractal dimensions from the rheological data of rennet casein gels of various concentrations and cooling

\* To whom correspondence should be addressed. Phone: 919-513-2092. Fax: 919-515-7124. E-mail: chris\_daubert@ncsu.edu.

<sup>†</sup> Department of Food Science.

<sup>‡</sup> Department of Chemical Engineering.

(1) Swaisgood, H. E. In *Food Chemistry*, 3rd ed.; Fenneman, O. R., Ed.; Marcel Dekker: New York, 1996; p 841.

(2) Swaisgood, H. E. *J. Dairy Sci.* **1993**, *76*, 3054–3061.

(3) Creamer, L. K.; MacGibbon, A. K. H. *Int. Dairy J.* **1996**, *6*, 539–568.

(4) Horne, D. S. *Int. Dairy J.* **1998**, *8*, 171–177.

(5) Walstra, P. *Int. Dairy J.* **1999**, *9*, 189–192.

(6) Fox, P. F.; Guinee, T. P.; Cogan, T. M.; McSweeney, P. H. *Fundamentals of Cheese Science*; ASPEN Publishers: Gaithersburg, MD, 2000.

(7) Carić, M.; Kaláb, M. In *Cheese: Chemistry, Physics and Microbiology*; Fox, P. F., Ed.; Chapman and Hall: New York, 1993; Vol. 2, p 467.

(8) Fox, P. F.; McSweeney, P. L. H. *Dairy Chemistry and Biochemistry*; Blackie Academic & Professional: New York, 1998.

(9) Bowland, E. L.; Foegeding, E. A. *J. Dairy Sci.* **2001**, *84*, 2372–2380.

(10) Lopez, C.; Bourgaux, C.; Lesieur, P.; Bernadou, S.; Keller, G.; Ollivon, M. *J. Colloid Interface Sci.* **2002**, *254*, 66–78.

(11) Campos, R.; Narine, S. S.; Marangoni, A. G. *Food Res. Int.* **2002**, *35*, 971–981.

(12) Tunick, M. H.; Nolan, E. J.; Shieh, J. J.; Basch, J. J.; Thompson, M. P.; Maleeff, B. E.; Holsinger, V. H. *J. Dairy Sci.* **1990**, *73*, 1671–1675.

(13) Bowland, E. L.; Foegeding, E. A. *J. Dairy Sci.* **1999**, *82*, 1851–1859.

(14) Dees, A. L. Effect of Various Ingredients on a Model Process Cheese System. M.S. Thesis, North Carolina State University, 2002.

(15) Shih, W.; Shih, W. Y.; Kim, S.; Liu, J.; Aksay, I. A. *Phys. Rev. A* **1990**, *42* (8), 4772–4779.

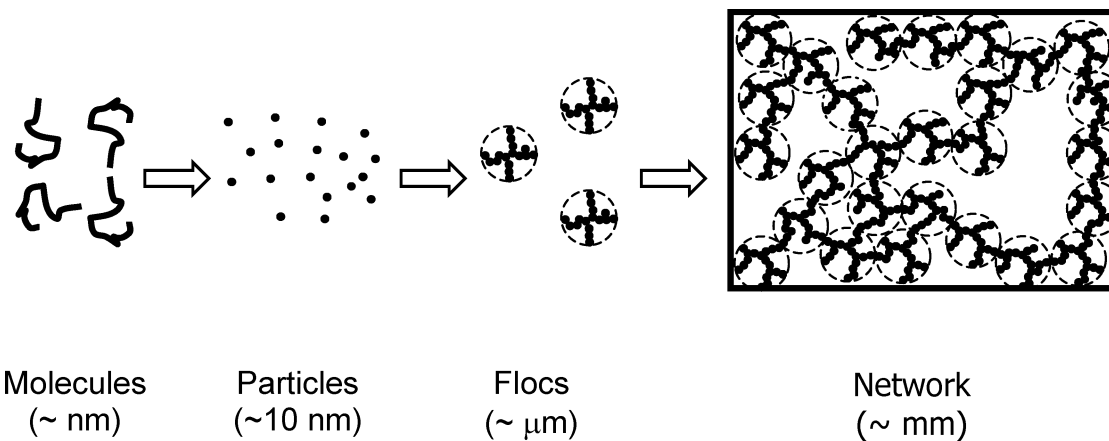


**Figure 1.** Schematic of the formation of rennet casein gels. The dashed circles are arbitrary boundaries of flocs, and the frame is an illustration of the occupied network space.

**Table 1. Formulation for Rennet Casein Gels**

amount (g)	rennet casein concentration (w/w)			
	18%	20%	22%	25%
NaH <sub>2</sub> PO <sub>4</sub>	0.60	0.60	0.60	0.60
Na <sub>2</sub> HPO <sub>4</sub>	5.00	5.00	5.00	5.00
NaCl	4.00	4.00	4.00	4.00
casein powder	36.00	40.00	44.00	50.00
deionized water	154.40	150.40	142.40	138.40

conditions. Studies in the second part of this paper describe the microstructure of a casein network, permitting the determination of floc sizes as a function of cooling rates.

### Materials and Methods

**Materials.** Rennet casein powder was purchased from New Zealand Milk Products (USA), Inc. (Lemoyne, PA). The protein content of the casein powder was determined by the Analytical Services Laboratory (Raleigh, NC) using a Perkin-Elmer PE 2400 CHN elemental analyzer (Perkin-Elmer Corp., Norwalk, CT). Casein powder had a nitrogen content of 12.78%, and therefore, the protein concentration was calculated to be 81.5% using a standard conversion factor. Food grade monosodium and disodium phosphates were kindly donated by Rhodia, Inc. (Cranbury, NJ), and salt (sodium chloride) was purchased from a local vendor.

**Gel Sample Preparation.** Rennet casein model gels were made according to the formulations in Table 1. Deionized water was heated to 50 °C, followed by the dissolution of all salts, and the solution pH was measured to be 7.2. Rennet casein powder was then dissolved into solution with a stirring bar rotating at 350 rpm. At this point, the sample appeared as a viscous paste and formed a gel upon overnight storage in a refrigerator at 5 °C.

**Rheological Measurements.** Small amplitude oscillatory tests were performed using a couette geometry and a Bohlin VOR rheometer (Bohlin Reologi, Inc., Cranbury, NJ). The bob (outer diameter, 2.5 cm) and cup (inner diameter, 2.7 cm) had serrated surfaces, minimizing slip at the walls. Initially, 14 g of the sample was loaded into the cup, and the opening was covered with Parafilm. Once the rheometer water bath reached 80 °C, the cup with the sample was loaded and incubated in the rheometer for 6 min at 80 °C to melt the gel. Next, the film was removed, and the bob was lowered into the measurement position. Excessive sample was removed, a layer of mineral oil was applied to the sample surface, and a sealed cap was placed on the cup to minimize moisture loss. The sample was equilibrated at 80 °C for 30 min and then cooled to 5 °C at four rates (0.025, 0.05, 0.1, and 0.5 °C/min). A 1% strain and an oscillation frequency of 0.05 Hz were used during cooling. Following oscillation, a strain sweep test was performed at a temperature of 5 °C and a frequency of 0.05 Hz after equilibrating for 30 min. All samples involved in the experiments were weighed before and after analysis to evaluate moisture loss.

### Fractal Theory and Fractal Dimension Determination.

Structure development of a globular protein system has been proposed to follow sequential steps at complementary length scales, from molecules to particles to flocs/aggregates and to a network.<sup>16–19</sup> For a heat-set whey protein gel, native proteins unfold upon heating, and the unfolded proteins aggregate into particles. Particles then aggregate into flocs, which form into a three-dimensional network throughout the total volume. Microscopy studies on particulate gels showed that protein aggregates are essentially spherical and much bigger than individual protein molecules.<sup>19–22</sup> Rennet casein network formation during cooling can also be described with three steps: (1) formation of particles from aggregated molecules, (2) flocculation of particles into flocs, and (3) development of a network from flocs (Figure 1).

Casein flocs are fractal objects that can be partially filled by the constructing units (particles), generating a fractal dimension ( $D_f$ ) that can be any value between 0 and 3. In this way, fractal dimension can be used to visualize the packing “compactness” of building elements in casein flocs: a larger value of  $D_f$  represents a more compact structure. The size ( $R_f$ ) of such a fractal object scales to the number of particles ( $N_p$ ) by<sup>23,24</sup>

$$N_p \propto (R_f/a)^{D_f} \quad (1)$$

where  $a$  is the representative particle diameter.

The application of fractal concepts in protein systems is still under development.<sup>20</sup> Fractal concepts can be used to describe the structure of pregel aggregates and are generally applied up to some length scale,<sup>25</sup> for example, the size of flocs.<sup>19</sup> At a scale larger than a floc, the flocs form a “nonfractal” network.

For a fractal object of a given amount of particles, the scaling equation (eq 1) is controlled by the interplay of the floc size and the fractal dimension. In a protein network, protein particles are building elements that can be “packed” in two different ways during aggregation: different compactness for flocs of similar sizes (Figure 2, A vs B) or different sizes for flocs of similar compactness (Figure 2, A vs C). When the particle number in a

(16) Richardson, R. K.; Ross-Murphy, S. B. *Int. J. Biol. Macromol.* **1981**, *3* (5), 315–322.

(17) Tobitani, A.; Ross-Murphy, S. B. *Macromolecules* **1997**, *30*, 4845–4854.

(18) Le Bon, C.; Nicolai, T.; Durand, D. *Macromolecules* **1999**, *32*, 6120–6127.

(19) Marangoni, A. G.; Barbut, S.; McGauley, S. E.; Marcone, M.; Narine, S. S. *Food Hydrocolloids* **2000**, *14*, 61–74.

(20) Verheul, M.; Roefs, S. P. F. M.; Mellema, J.; de Kruif, K. G. *Langmuir* **1998**, *14*, 2263–2268.

(21) Ju, Z. Y.; Kilara, A. *J. Agric. Food Chem.* **1998**, *46*, 1830–1835.

(22) Ju, Z. Y.; Kilara, A. *J. Dairy Sci.* **1998**, *81*, 1236–1243.

(23) Bremer, L. G. B.; Bijsterbosch, B. H.; Schrijvers, R.; van Vliet, T.; Walstra, P. *Colloids Surf.* **1990**, *51*, 159–170.

(24) Bremer, L. G. B.; Bijsterbosch, B. H.; Walstra, P.; van Vliet, T. *Adv. Colloid Interface Sci.* **1993**, *46*, 117–128.

(25) Gosal, W. S.; Ross-Murphy, S. B. *Curr. Opin. Colloid Interface Sci.* **2000**, *5*, 188–194.

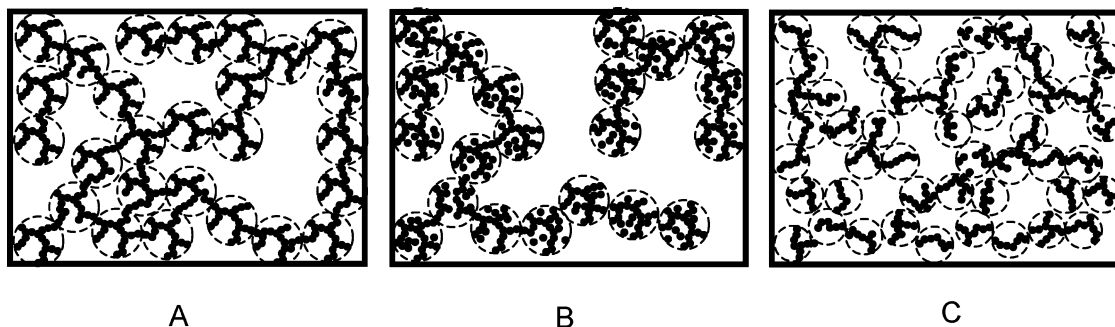


**Figure 2.** Fractal dimension (A vs B) and floc size (A vs C) effects on a gel structure. The filled small circles stand for protein particles, the dashed circles are arbitrary boundaries of flocs, and the frame is an illustration of the network space occupied.

floc is increased, the fractal dimension increases, and the floc population is reduced. When the floc size is shrunk, the total number of flocs is greater at a similar degree of compactness.

The aggregation of protein particles is controlled by colloidal interactions. In the classical Derjaguin–Landau–Verwey–Overbeek (DLVO) theory, the interplay between repulsive charge–charge interactions and attractive dispersion interactions describes the stability of a colloidal system.<sup>26</sup> Once aggregated, particles stay at a separation corresponding to the energy minimum.<sup>27</sup> In a globular protein gel, the interactions are usually more complex than the DLVO forces. The complexity arises from complicated short-range, non-DLVO forces such as hydration forces, hydrogen bonding, and hydrophobic interactions. The gels formed by such physical forces, for example, rennet casein gels, are called physical (particle) gels, while chemical (polymer) gels involve covalent bonds.<sup>28</sup>

Particle gels and polymer gels are similar, as flocs in a particle gel are analogous to “blobs” in a polymer gel.<sup>15</sup> On the basis of this analogy, Shih et al.<sup>15</sup> developed a scaling theory following Brown,<sup>29</sup> Buscall et al.,<sup>30</sup> and Kantor and Webman.<sup>31</sup> Bremer et al.<sup>23,24</sup> independently developed a scaling theory by intuitively classifying the stress-carrying strands in flocs to be straight or hinged, which was further elaborated by Mellema et al.<sup>32</sup> to exist as five types: random, curved, hinged, straight, and rigid. The curved and rigid strands were consistent with the categories proposed by Shih et al. To identify a strand type according to Mellema et al., however, one needs specific parameters from various techniques other than rheological ones, such as fractal dimension from microscopy images. Despite a detailed analysis, Mellema et al. found it difficult to analyze casein gels at pH 5.3 and 30 °C, which was argued to have been caused by rearrangement during aging.

Studying a particle gel with the approach proposed by Shih et al. only requires rheological data, and the fractal dimensions estimated from the model were similar to those from light scattering and microscopy approaches when applied to protein gels, such as bovine serum albumin,  $\beta$ -lactoglobulin, 11S soybean globulin, whey protein isolate, and caseinate gels.<sup>19,33–37</sup> This

model was also successfully applied to fat crystals of high volume fractals (70%),<sup>38</sup> as demonstrated by similar fractal dimensions determined from the scaling theory and polarized light microscopy. An analogy was made between fat crystal microstructure after cooling and colloidal flocs, which has since been applied to a variety of complex food systems.<sup>39,40</sup>

According to Shih’s model, a colloidal gel is described as closely packed fractal flocs. The links between the flocs are categorized into two regimes: the strong-link regime (the links between flocs being stronger than the links within flocs) and the weak-link regime (the links between flocs being weaker than the links within flocs). The elastic constant ( $K$ ) and the limit of the linear viscoelastic regime (LVR,  $\gamma_0$ ) are scaled to the volume fraction ( $\phi$ ) by eqs 2 and 3 for the strong-link regime and eqs 4 and 5 for the weak-link regime. As substantiated by eqs 3 and 5, a decrease in the limit of the LVR with an increase in volume fraction can be used to identify a system within the strong-link regime, while the opposite scenario prevails for the weak-link regime.

$$K \propto \phi^{(3+x)/(3-D)} \quad (2)$$

$$\gamma_0 \propto \phi^{-(1+x)/(3-D)} \quad (3)$$

$$K \propto \phi^{1/(3-D)} \quad (4)$$

$$\gamma_0 \propto \phi^{1/(3-D)} \quad (5)$$

Here,  $x$  is the backbone fractal dimension of the flocs, varying between 1.0 and 1.3.

To determine the fractal dimensions of rennet casein gels cooled at different rates, small amplitude oscillatory tests were used to collect rheological data from casein gels at four concentrations, each cooled at four different rates. Following cooling, strain sweep tests identified the model casein system to be within the strong-link or weak-link regime. Storage moduli were then used to estimate the fractal dimension as a function of cooling rate.

## Results and Discussion

**Rheology Data.** Similar to industrial observations of the cooling effects on processed cheese, casein gels showed a smaller storage modulus ( $G'$ ) during cooling at faster rates. The rheological data for 25 and 18% rennet casein gels during cooling are presented in Figure 3, and the trends were the same at the other concentrations (22 and 20%). The storage modulus also increased with an increase in casein concentration and a decrease in temperature. All strain sweep tests demonstrated a limit of the LVR higher than 1% at different cooling rates for all concentrations (see Figure 4 for 25 and 18% rennet casein gels).

Strain sweep data for 25% rennet casein gels at 5 °C cooled at different rates are presented in Figure 4. Besides

(38) Narine, S. S.; Marangoni, A. G. *Phys. Rev. E* **1999**, *59*(2), 1908–1920.

(39) Liu, Z.; Scanlon, M. G. *Food Bioprod. Process.* **2003**, *81* (c3), 224–238.

(40) Hagiwara, T.; Wang, H. L.; Suzuki, T.; Takai, R. *J. Agric. Food Chem.* **2002**, *50* (11), 3085–3089.

(26) Verwey, E. J. W.; Overbeek, J. T. G. *Theory of Stability of Lyophobic Colloids*; Elsevier: Amsterdam, The Netherlands, 1948.

(27) Israelachvili, J. N. *Intermolecular and Surface Forces*, 2nd ed.; Academic Press: San Diego, CA, 1992.

(28) Ross-Murphy, S. B. *J. Texture Stud.* **1995**, *26*, 391–400.

(29) Brown, W. D. *The Structure and Physical Properties of Flocculating Colloids*. Ph.D. Dissertation, University of Cambridge, Cambridge, England, 1987.

(30) Buscall, R.; Mills, P. D. A.; Goodwin, J. W.; Lawson, D. W. *J. Chem. Soc., Faraday Trans. 1* **1988**, *84*, 4249–4260.

(31) Kantor, Y.; Webman, I. *Phys. Rev. Lett.* **1984**, *52* (21), 1891–1894.

(32) Mellema, M.; van Opheusden, J. H. J.; van Vliet, T. *J. Rheol.* **2002**, *46* (1), 11–29.

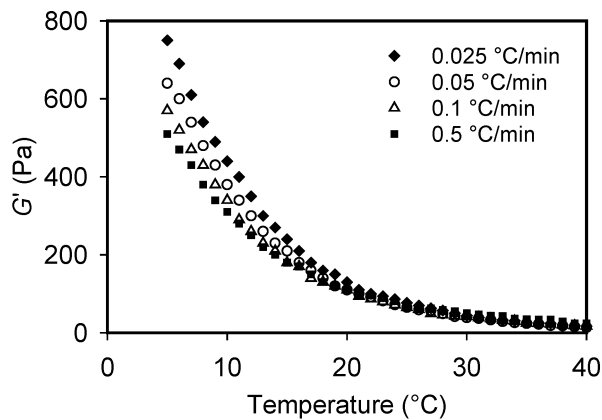
(33) Hagiwara, T.; Kumagai, H.; Matsunaga, T. *J. Agric. Food Chem.* **1997**, *45*, 3807–3812.

(34) Hagiwara, T.; Kumagai, H.; Matsunaga, T.; Nakamura, K. *Biosci. Biotechnol. Biochem.* **1997**, *61* (10), 1663–1667.

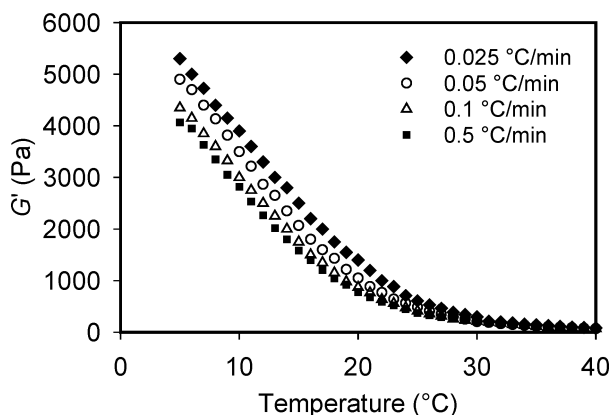
(35) Hagiwara, T.; Kumagai, H.; Nakamura, K. *Food Hydrocolloids* **1998**, *12*, 29–36.

(36) Ikeda, S.; Foegeding, E. A.; Hagiwara, T. *Langmuir* **1999**, *15*, 8584–8589.

(37) Vreeker, R.; Hoekstra, L. L.; den Boer, D. C.; Agterof, W. G. M. *Food Hydrocolloids* **1992**, *6* (5), 423–435.



(a)



(b)

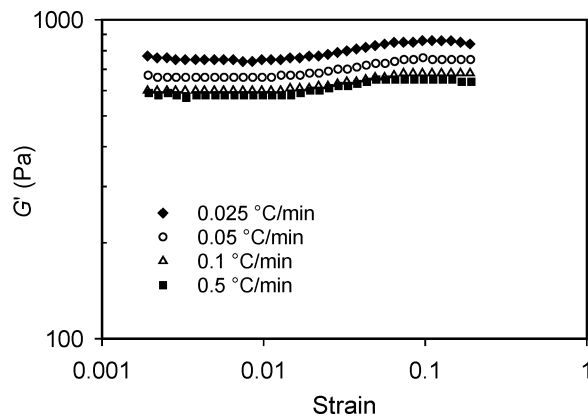
**Figure 3.** Storage moduli of 18% (a) and 25% (b) rennet casein gels during cooling at different rates.

a smaller limit of the LVR, gels cooled slower showed a higher  $G'$  value. Thus, a slower cooling rate delivered a firmer and more brittle gel. At a strain beyond the LVR, all gels displayed the same storage modulus.

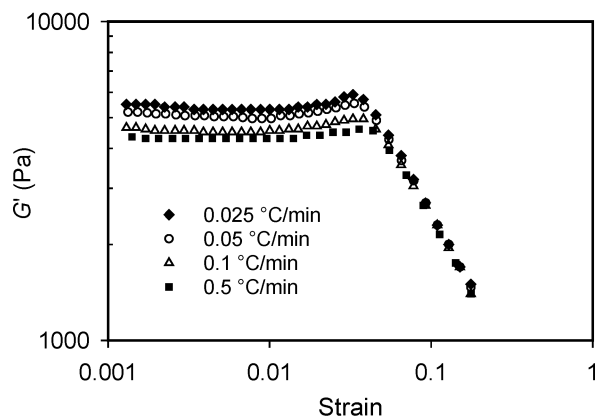
Moisture analysis results were not affected by the length of the test time at different cooling rates, eliminating the possible increase in storage modulus as a result of sample dehydration. The differences in rheological properties and protein functionality were attributed to microstructural differences induced by the cooling process.

**Fractal Dimension of Casein Flocs.** Except for an apparent limit of linear viscoelasticity at a concentration of 25%, the strain sweep tests did not enable the identification of an upper limit to the LVR, as the storage moduli of these gels did not decrease at the maximum strain (20%) limited by the rheometer (Figure 4). Therefore, the LVR limit increased with a decrease in concentration, and the system was characterized as being within the strong-link regime according to eq 3. The fractal dimension can therefore be calculated by eq 2. The storage moduli of casein gels at the end of cooling are presented in Figure 5 and regressed using a power-law model, similar to Ikeda et al.<sup>36</sup> Similar exponents ( $\sim 6.3$ ) were found at four cooling rates, and the calculated fractal dimensions were  $\sim 2.35$  (Table 2). Therefore, the flocs within the casein gels had a similar degree of compactness when cooled at different rates.

**Fractal Dimensions as Determined by Colloidal Interactions.** The aggregation of colloidal particles is determined by the overall interaction energy contributed from different types of forces. Once aggregated, the



(a)



(b)

**Figure 4.** Strain sweep of 18% (a) and 25% (b) rennet casein gels at 5 °C cooled at different rates.

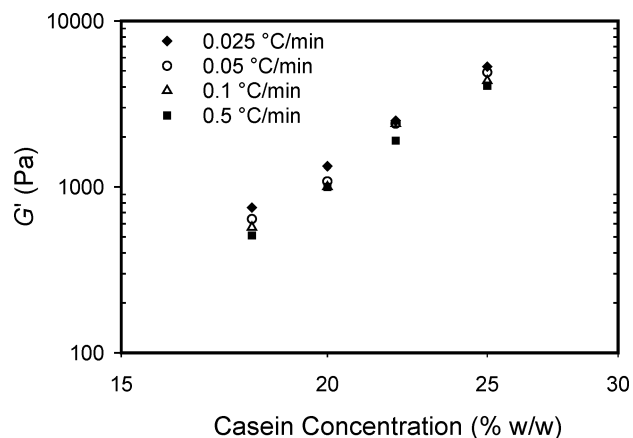


**Figure 5.** Storage moduli of rennet casein gels at 5 °C cooled at different rates.

**Table 2. Fractal Dimensions of Rennet Casein Flocs as a Function of Cooling Rate Calculated by the Scaling Theory<sup>15</sup>**

cooling rate (°C/min)	fractal dimension
0.5	2.35
0.1	2.36
0.05	2.36
0.025	2.32

particles stay at their minimal separation distance determined by the (primary) energy minimum between the particles.<sup>27</sup> The depth of the energy minimum determines the life of the aggregate. If the attractive force is

not strong enough, the process may be reversible.<sup>41</sup> If the energy minimum cannot be overcome by a process such as heating, the particles cannot be separated and the process is irreversible.

In DLVO theory, colloidal stability is determined by the interplay of the attractive van der Waals forces and the repulsive electrostatic interactions.<sup>27</sup> The van der Waals interaction between two identical spheres can be estimated by eq 6,<sup>42</sup> and the electrostatic interaction can be estimated by eq 7 for a constant surface potential lower than 25 mV:<sup>27</sup>

$$W_{\text{vdw}} = -\frac{A}{6} \left( \frac{2a^2}{r^2 - 4a^2} + \frac{2a^2}{r^2} + \ln \left( \frac{r^2 - 4a^2}{r^2} \right) \right) \quad (6)$$

$$W_{\text{er}} = \frac{2\pi a \sigma^2}{\epsilon \epsilon_0 \kappa^2} \exp(-\kappa h) \quad (7)$$

where  $A$  is the Hamaker constant,  $a$  is the particle radius,  $r$  is the center-to-center distance,  $\sigma$  is the surface charge density,  $h$  is the separation between the spheres ( $h = r - 2a$ ),  $\kappa$  is the Debye length, and  $\epsilon$  and  $\epsilon_0$  are the relative permittivity of the solvent and that of the free space, respectively. The relative permittivity of water as a function of the absolute temperature ( $T$ ) can be expressed as<sup>43</sup>

$$\epsilon(T) = 249.21 - 0.79069T + 0.00072997T^2 \quad (8)$$

The Hamaker constant for protein particles dispersed in a solvent may be determined by the Lifshitz approach or surface thermodynamics.<sup>44</sup> The Hamaker constants of other milk proteins such as bovine serum albumin<sup>45</sup> and  $\beta$ -lactoglobulin<sup>46</sup> have been computed to be  $3.10k_B T$  and  $5k_B T$ , respectively, where  $k_B$  is the Boltzmann constant. Using low-angle laser-light scattering, Coen et al.<sup>47</sup> determined a pH-independent Hamaker constant of  $\sim 10k_B T$  at an ionic concentration of 1.0 M. A Hamaker constant of  $6k_B T$  has been used to calculate the van der Waals interactions in this work.

Among the parameters in electrostatic interactions, the net charge of a casein mixture at pH 7.2 is  $\sim -12.7$ , estimated from the Henderson–Hasselbalch equation by summing charges from all amino acid residues.<sup>2</sup> The Debye length was estimated to be 0.28 nm ( $\kappa^{-1} = 3.288\sqrt{I} \text{ nm}^{-1}$ , where  $I$  is the ionic concentration in M estimated from the salt concentrations in Table 1), indicating that the electrostatic interaction was significant only at a very short separation distance.

Using these parameters, the interactions were calculated as a function of the separation distance referenced to  $k_B T$  (Figure 6). van der Waals interactions always dominated electrostatic interactions, as estimated for many protein systems at high salt concentrations.<sup>48–51</sup> This response suggests other types of forces are stabilizing the caseins at high temperatures.

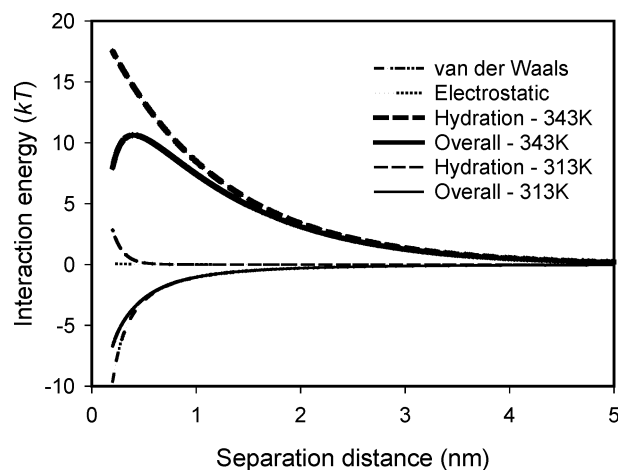


**Figure 6.** Interaction energies ( $W$ s) between casein particles as a function of separation at two temperatures.

Besides DLVO forces, other forces existing in a protein system include hydrogen bonding, hydrophobic interactions, and hydration forces.<sup>27</sup> The hydration force is a strong repulsive force resulting from the structure of water molecules<sup>27</sup> or from overlapping hydrated counterions on the protein surface.<sup>52</sup> Experiments have demonstrated an oscillatory, repulsive hydration force between two rigid and smooth surfaces with a period equivalent to the diameter of water molecules.<sup>27</sup> The oscillatory, repulsive hydration force, however, is not applicable to a biosystem whose surface is usually flexible.<sup>41,53</sup>

Since a protein particle surface has groups protruding into the solution, the overlapping of these groups from two protein particle surfaces provides a steric-hydration force that stabilizes the protein.<sup>41</sup> The steric-hydration energy ( $W_{\text{hd}}$ ) per unit area is empirically written in an exponential decay format (eq 9).

$$W_{\text{hd}} = 3\Gamma k_B T \exp(-h/\lambda_0) \quad (9)$$

where  $\Gamma$  is the surface density of protruding molecules in units of  $\text{m}^{-2}$  and  $\lambda_0$  is the characteristic decay length.

The hydration forces originate from the decrease in entropy when two surfaces start overlapping, and  $\lambda_0$  ranges typically from 0.1 to 1.1 nm.<sup>27,54</sup> The aforementioned parameters have been correlated with rheological data by Ikeda and Nishinari,<sup>49,50</sup> but the estimated hydration force was effective at a separation distance up to 25 nm, which was far beyond the range where a repulsive hydration force could be effective.

Despite the challenges in quantification, the steric-hydration force provides a qualitative explanation for the stability of the model rennet casein system, because casein molecules are flexible.<sup>55,56</sup> At a high temperature, the

(41) Leckband, D.; Israelachvili, J. *Q. Rev. Biophys.* **2001**, *34* (2), 105–267.

(42) Russel, W. B.; Saville, D. A.; Schowalter, W. R. *Colloidal Dispersions*; Cambridge University Press: New York, 1989.

(43) *CRC Handbook of Chemistry and Physics*, 83rd ed.; Lide, D. R., Ed.; CRC Press: Cleveland, OH, 2002.

(44) Molina-Bolívar, J. A.; Galisteo-González, F.; Hidalgo-Álvarez, R. *J. Chem. Phys.* **1999**, *110* (11), 5412–5420.

(45) Roth, C. M.; Neal, B. L.; Lenhoff, A. M. *Biophys. J.* **1996**, *70*, 977–987.

(46) Schaink, H. M.; Smit, J. A. M. *Phys. Chem. Chem. Phys.* **2000**, *2*, 1537–1541.

(47) Coen, C. J.; Blanch, H. W.; Prausnitz, J. M. *AIChE J.* **1995**, *41* (4), 996–1004.

(48) Beretta, S.; Chirico, G.; Baldini, G. *Macromolecules* **2000**, *33*, 8663–8670.

(49) Ikeda, S.; Nishinari, K. *Biomacromolecules* **2000**, *1*, 757–763.

(50) Ikeda, S.; Nishinari, K. *Int. J. Biol. Macromol.* **2001**, *28*, 315–320.

(51) Petsev, D. N.; Vekilov, P. G. *Phys. Rev. Lett.* **2000**, *84* (6), 1339–1342.

(52) Paunov, V. N.; Kaler, E. W.; Sandler, S. I.; Petsev, D. N. *J. Colloid Interface Sci.* **2001**, *240*, 640–643.

(53) Israelachvili, J.; Wennerström, H. *Nature* **1996**, *379* (18), 219–225.

(54) Molina-Bolívar, J. A.; Ortega-Vinuesa, J. L. *Langmuir* **1999**, *15*, 2644–2653.

(55) Andrews, A. L.; Atkinson, D.; Evans, M. T. A.; Finer, E. G.; Green, J. P.; Phillips, M. C.; Robertson, R. N. *Biopolymers* **1979**, *18*, 1105–1121.

(56) Holt, C.; Sawyer, L. *J. Chem. Soc., Faraday Trans. 1* **1993**, *89* (15), 2683–2692.

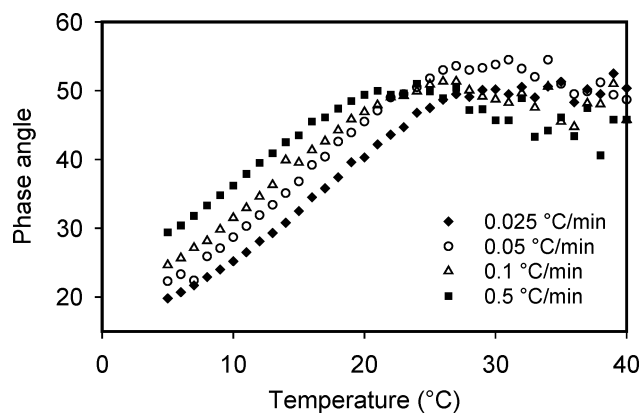


**Figure 7.** Phase angles of 25% rennet casein gels during cooling at different rates.

flexible surface provides an entropy-driven repulsive force, preventing the aggregation of casein particles. On the other hand, the repulsive force becomes less significant upon cooling because the motion of the surface is weaker at a lower temperature. At a “critical” temperature, the attractive van der Waals force becomes predominant, and protein particles aggregate into flocs and are separated at a distance corresponding to the primary energy minimum. To describe this process, a value of  $2.2 \times 10^{16} \text{ m}^{-2}$  was assigned to  $\Gamma$  and 1.1 nm to  $\lambda_0$  at a high temperature (70 °C). Summation of the van der Waals, electrostatic, and steric-hydration forces demonstrated an energy barrier greater than  $10k_B T$ , meaning protein particles are stable at this temperature (Figure 6). On the other hand, the slower motion of protruding molecules dictates a shorter effective distance for the steric-hydration force at lower temperatures. For example, by letting  $\lambda_0$  be 0.1 nm and keeping the value of  $\Gamma$  constant (same amount of protruding molecules) at 40 °C, the overall energy becomes attractive at all separations (Figure 6), indicating protein particles are unstable at this temperature.

Once aggregation occurs, the minimum separation distance between the casein particles in flocs is determined by surface characteristics. For all systems at a constant protein concentration, the colloidal interaction energies were the same at different cooling schedules, because the samples had the same chemical compositions, resulting in a similar separation distance between particles. This separation distance, together with similar particle sizes at identical compositions, determines the compactness of fractal flocs and their fractal dimensions, as estimated in the previous section.

**Effect of Cooling Rates on the Gelation Temperatures.** Despite different ways for defining the onset of gelation, a phase angle of 45° is commonly applied as a criterion.<sup>28</sup> After the crossover, the storage modulus dominates over the loss modulus and the phase angle is always smaller than 45°. An example of phase angle evolution during cooling is shown in Figure 7 for 25% rennet casein gels, and a decrease in gelation temperature was observed as the cooling rate was increased. The trend was the same for all concentrations. As gelation is an indication of cross-linking of flocs, cross-linking of flocs occurred at a higher temperature when cooled at a slower rate.

Floc formation starts with the aggregation of two particles into a doublet, followed by the addition of other particles.<sup>42</sup> At a slower cooling rate, protein particles spend more time in the temperature range favorable for doublet formation. More doublets were thus formed, providing more sites for floc growth. The completion of floc formation

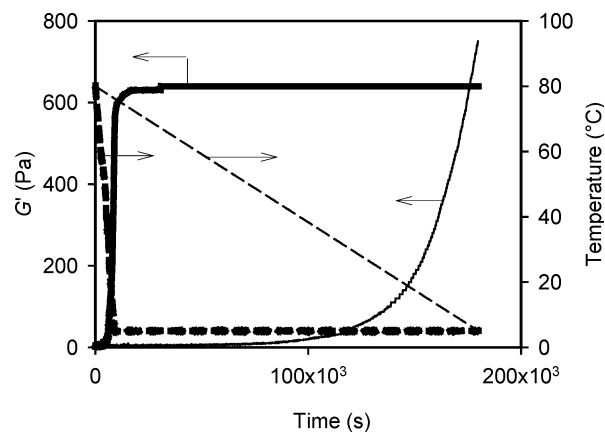


**Figure 8.** Storage moduli of 18% rennet casein gels when cooled at 0.025 °C/min (thin lines) and 0.5 °C/min followed by incubation at 5 °C (thick lines). The solid lines are for storage moduli, and the dashed lines are for temperatures.

occurred at a higher temperature once all protein particles were consumed into more smaller-sized flocs, as demonstrated by higher gelation temperatures during cooling at slower rates. More smaller-sized flocs eventually created more cross-links among the network, as demonstrated by higher storage moduli during slower cooling processes (Figure 3).

**Cooling Rate Effects versus Aging Effects.** At a slower cooling rate, rennet casein systems spend more time cooling after gelation. There was a need to distinguish cooling rate effects from time effects or aging effects because some protein systems demonstrated an increase in the storage modulus with time after gelation at a constant temperature.<sup>20</sup> To address this issue, an additional test was performed by first cooling an 18% rennet casein gel at 0.5 °C/min from 80 to 5 °C and subsequently incubating at 5 °C for a total test time equaling that used during a cooling rate of 0.025 °C/min. During the incubation at 5 °C, the storage modulus increased slightly and remained at a final value lower than that cooled at 0.025 °C/min (Figure 8). The aging effects were different from the cooling effects; otherwise, the final storage moduli would be the same if treated for similar cooling periods.

In the second part of this study, microscopy experiments were performed on the gel after incubation at 5 °C. There was no difference in the visual appearance, floc size, or floc distribution for the gels cooled at 0.5 °C/min with or without incubation. During incubation, idle flocs connected to the network, strengthening the gel. Once these flocs were integrated into the network, the gel could not be further strengthened. The cooling rate therefore affected the floc size, and aging enabled the connection of idle flocs.

## Conclusions

Slower cooling rates generated stronger rennet casein gels, hypothesized here to be a result of a greater degree of cross-linking among flocs. The number of flocs and thus cross-links is proposed to be a function of floc fractal dimension and size. Floc fractal dimensions were similar at different cooling schedules due to identical interactions. A stronger gel at a slower cooling rate resulted from a greater amount of smaller flocs (thus more cross-links). Formation of more smaller-sized flocs was completed at a higher temperature during slower cooling, enabling gelation at a higher temperature when connecting individual flocs into a network. Additionally, cooling effects differed from aging effects, which demonstrated a slight

increase in the storage modulus following the cooling at a faster rate due to the bonding of idle flocs into the network.

**Acknowledgment.** This study was conducted on the basis of funding received partly from the Southeast Dairy Foods Research Center and partly from the North Carolina Agricultural Research Service, resulting in the publication of Paper No. FSR-03-37 of the Journal Series of the Department of Food Science, North Carolina State Uni-

versity, Raleigh, NC. The authors are grateful for the technical support from Dr. Van Den Truong. The use of trade names in this publication does not imply endorsement by the North Carolina Agricultural Research Service of the products named nor criticism of similar ones not mentioned. Paper No. FSR-03-37 of the Journal Series of the Department of Food Science, North Carolina State University, Raleigh, NC 27695-7624.

LA036147W